Francesca Cigna · Silvia Bianchini · Nicola Casagli

How to assess landslide activity and intensity with Persistent Scatterer Interferometry (PSI): the PSI-based matrix approach

Abstract We provide a step-by-step analysis and discussion of the 'PSI-based matrix approach', a methodology employing ground deformation velocities derived through Persistent Scatterer Interferometry (PSI) for the assessment of the state of activity and intensity of extremely to very slow landslides. Two matrices based on PSI data are designed respectively for landslides already mapped in preexisting inventories and for newly identified phenomena. Conversely, a unique intensity scale is proposed indiscriminately for both. Major influencing factors of the approach are brought to light by the application in the 14km² area of Verbicaro, in Northern Calabria (Italy). These include lack of PSI data within the landslide boundaries, temporal coverage of the available estimates, and need of field checks as well as the operative procedures to set the activity and intensity thresholds. For the area of Verbicaro, we exploit 1992–2011 PSI data from ERS1/2 and RADARSAT1/2 satellites, projecting them along the maximum slope directions. An activity threshold of ±5mm/year is determined by applying the average projection factor of local slopes to the PSI data precision. The intensity threshold between extremely and very slow phenomena (16mm/year) is reduced by ~20% to account for temporal and spatial averages being applied to attribute representative velocities to each landslide. The methodology allows assessing the state of activity and the intensity for 13 of the 24 landslides premapped in the 2007 inventory and for two newly identified phenomena. Current limitations due to characteristics and spatial coverage of PSI data are critically tackled within the discussion, jointly with respective implications.

Keywords Landslide · Persistent Scatterer Interferometry · State of activity · Intensity · SAR Interferometry · PSI-based matrix

Introduction

In many countries of the world, landslide hazard is one of the major causes of life losses, injuries, and damages to private and public structures and infrastructure (WP/WLI 1993). Identifying and mapping these phenomena is essential to reduce their social and economic impacts and for the consequent improvement of future urban expansion and planning strategies. Inventory maps address the identification of landslide processes and include location, geometrical parameters (e.g., volume and total length or area), type, causal factors, activity, and intensity of each landslide within an investigated territory. The information reported within these maps represent crucial and priority factors for every landslide hazard or risk study, since they facilitate the assessment of the spatial and temporal frequencies of landslides and a better understanding of susceptibility and vulnerability.

In hilly and mountainous areas, on-site methods for the analysis of slope instability are not always economically and practically suitable for carrying out a systematic investigation of landslide phenomena at the regional scale because of both huge extension of observed areas and frequently, difficult accessibility. Integrating and complementing conventional investigations with remote sensing techniques represent a valuable support for landslide mapping due to wide area coverage, noninvasiveness, and cost-effectiveness of remotely sensed data. Some innovative methodologies for the assessment of landslide activity through aerial photointerpretation have been carried out in the last years (Canuti and Focardi 1986; Gonzalez-Diez et al. 1999; Guzzetti et al. 1999; Parise and Wasowski 1999; Wieczorek 1984); however, they suffer from significant uncertainties due to the subjectivity in the activity evaluation and difficulties in the recognizability of landslide-related geomorphic features and in the quantification of the observed land changes, especially for urban and suburban environments. As well as for the state of activity, many difficulties are usually encountered during the evaluation of landslide intensity (Hungr 1997; i.e., destructiveness of a landslide, in terms of kinetic energy, volume, area, depth, movement velocity or total displacement, etc.), due to the lack of a single standardized procedure for the quantification of this parameter (e.g., Lateltin et al. 2005; Uzielli et al. 2008). Moreover, when investigating very large areas affected by a variety of different phenomena, retrieving detailed information about volume, kinetic energy or velocity it is—more often than not—difficult and time-consuming.

A new methodology for the updating of landslide inventories has been recently experimented by the scientific community (e.g., Cascini et al. 2010; Farina et al. 2006; Herrera et al. 2010; Meisina et al. 2006; Notti et al. 2010; Righini et al. 2011). This methodology couples conventional thematic data (e.g., topographic, geological, land use maps, and optical images) and on-site investigations with ground deformation estimates obtained through Persistent Scatterer Interferometry (PSI) analyses (e.g., Crosetto et al. 2010). It generally operates at medium or large scales (i.e., 1:100,000–1:25,000 and 1:25,000–1:5,000, respectively; Fell et al. 2008), and its contributions consist in (Fig. 1): (i) detection of geomorphologic phenomena not emerging from conventional analyses, field surveys, or bibliographic studies; (ii) verification or modification of landslide boundaries; (iii) assessment of landslide velocity and intensity; and (iv) evaluation of state of activity.

Bianchini et al. (2012) give an overview of the whole methodology and assign it the name 'Landslide HotSpot Mapping' (LHSM) to refer to its capability of scanning wide areas and identifying narrow unstable zones characterized by higher landslide hazard. Treasuring of the above-mentioned applications and their findings, this study focuses on the improvement and standardization of the procedure for the assessment of the landslide state of activity and intensity, which represents a crucial phase of the LHSM methodology. To define this procedure, we coin the name 'PSI-based matrix approach' and provide a detailed and step-by-step analysis and discussion of its operational chain. The potentials of the

Fig. 1 Methodology for the updating of inventory maps and the assessment of state of activity and intensity of slow-moving landslides exploiting the PSI-based matrix approach
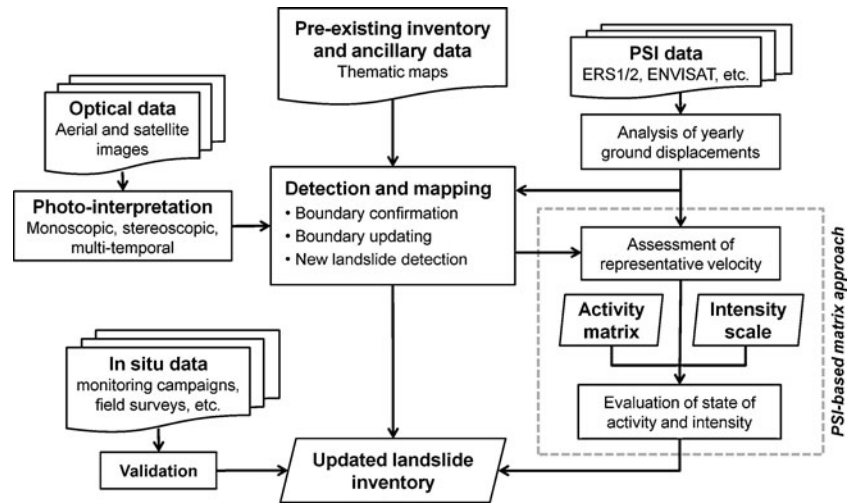
methodology are also shown through the example of Verbicaro (Italy), for which the preexisting landslide inventory is updated using PSI-derived 1992–2011 data from ERS1/2 and RADARSAT1/2 satellites.

PSI-based matrix approach

Since the beginning of the 21st century, Synthetic Aperture Radar Interferometry (InSAR) and PSI techniques are demonstrating their potential for detecting land motions through the analysis of long temporal series of satellite SAR images. Results of PSI processing are sparse grids of radar targets (the so-called Persistent Scatterers, PS), for which the following information are generally provided: Line Of Sight (LOS) estimates of yearly motion rates (i.e., millimeters per year), time series of deformation-acquisition by acquisition (i.e., millimeters), and quality parameters such as PS coherence as well as velocity and height standard deviations (e.g., Crosetto et al. 2010; Ferretti et al. 2001; Werner et al. 2003). Both historical archives of SAR images (e.g., ERS1/2 and JERS data) and currently operational missions (e.g., Envisat, Radarsat1/2, TerraSAR-X, and COSMO-SkyMed) can be exploited to analyze past and recent ground displacements and reconstruct the deformation history of the observed scene with millimeter precision.

PSI-based investigations of natural hazards and, in particular, landslide processes, are successfully being carried out in the last years, demonstrating the flexibility of these techniques to different landslide typologies and dimensions, thanks to their high spatial and temporal resolutions, multitemporal scalability, integrability, and interoperability with conventional on-site investigations (e.g., Bovenga et al. 2006; Cascini et al. 2010; Colesanti and Wasowski 2006; Farina et al. 2006; Herrera et al. 2010; Hilley et al. 2004).

Definition and applicability

The 'PSI-based matrix approach' is a methodology for the assessment (or updating) of the landslide state of activity and intensity, which exploits PSI-derived multitemporal estimates of ground deformation as indicators of activity and magnitude of landslide processes. This approach uses a simplified version of the official classification of the states of activity defined in the multilingual landslide glossary (WP/WLI 1993), distinguishing the following four classes of activity:

– 'Stabilized' (S), not affected by their original causes anymore;
– 'Dormant' (D), potentially being reactivated;
– 'Active' (A), currently moving;
– 'Reactivated' (R), moving after being inactive.

The first two classes are included in the inactive one, comprising all phenomena which did not move in the last 12 months. The stabilized class includes both the artificially stabilized phenomena (artificially protected from their causes through remedial measures) and the naturally stabilized ones, i.e., abandoned (no longer affected by their original causes) and relict (developed under different climatic and geomorphologic conditions from the current ones) landslides. Suspended landslides (moved in the last 12 months but not moving at present) are incorporated in the active class.

With regard to the intensity (Hungr 1997), the PSI-based matrix approach considers the landslide potential to cause damage in terms of movement velocity, exploiting the velocity classification of Cruden and Varnes (1996). Due to the main intrinsic characteristic of PSI-derived estimates—some of which are analyzed critically within the discussion—the methodology is currently applicable just to the classes of Extremely Slow (ES) and Very Slow (VS) movements ($V < 16$ mm/year and 16 mm/year $\leq V < 1.6$ m/year, respectively). This limitation influences also the applicability of the PSI-based methodology in terms of landslide typology, restricting its range to the analysis of phenomena with very slow dynamics, such as deep-seated gravitational slope deformations, creep, and, just partially, rototranslational slides, flows, and complex landslides, as long as their velocities do not overcome the above-mentioned rates.

As observed by Colesanti and Wasowski (2006), landslide-induced displacements detectable through PSI techniques mainly concern postfailure residual deformation and landslide reactivations involving naturally degraded slopes and preexisting shear surfaces. These movements are very suitable to analysis through PSI techniques, since they usually evolve with very low velocities (few tens of centimeters per year) with respect to first-time activations and generally persist over long time periods (several years).

Landslide representative velocity

The evaluation of spatial distribution and boundaries of landslide phenomena within the investigated area represents the preparatory phase of the PSI-based matrix approach (Fig. 1). This step, which is not tackled inside the present paper, can be carried out through conventional geomorphologic approaches, photointerpretation, and even the support from PSI data (e.g., Bianchini et al. 2012; Meisina et al. 2008; Righini et al. 2011). Once this preparatory phase is completed, the PSI-based matrix approach starts with the estimation of landslide representative velocities.

The ideal situation for the implementation of this approach is the availability of two or more sets of PSI data acquired over different monitoring intervals; this requirement enables the analysis of the evolution of the deformational behavior of the observed phenomena by comparing velocities and trends between different time spans. The availability of SAR archives responds to this need by providing long temporal stacks of satellite radar imagery for many areas of the Earth's surface and thereby facilitating the understanding of landslide behaviors, distributions of activity (e.g., advancing, retrogressive, enlarging, and diminishing), and states of activity. For the identification of the latter, the possibility of comparing the status and evolution of ground motions in time is a fundamental requirement.

Assuming the availability of both past and recent PSI-derived data, two (or more) different time spans can be considered for the analysis: the historical and present intervals, whose respective temporal coverages can be defined as $[D_{H_1}–D_{H_2}]$ and $[D_{P_1}–D_{P_2}]$. The historical and present representative velocities of each landslide, V_H and V_P, will be evaluated through the analysis of the available PSI data in the $[D_{H_1}–D_{H_2}]$ and $[D_{P_1}–D_{P_2}]$ periods respectively, e.g., using ERS1/2 [1992–2001] and ENVISAT [2002–2010] PSI data. Separately for the evaluation of the V_H and V_P the spatial distribution, number, and density δ (i.e., Persistent Scatterers per square kilometer) of radar targets identified inside the boundary of each landslide are analyzed (Fig. 1). A reliable and robust interpretation of landslide motion rates is usually focused only on those phenomena with a minimum density of targets of about 20–30 PS/km²; this is done to increase the reliability of the representative velocity evaluations (Notti et al. 2010). Anyway, this density threshold depends on the PSI data source and, in particular, the spatial resolution of the processed SAR images. In any case, regardless of the landslide spatial extension, at least three to five radar targets should be considered for such an analysis because data retrieved on single targets may not be indicative of a real landslide process but more likely due to single instable structures, e.g., building settlement (Meisina et al. 2008; Notti et al. 2010).

Usually, a simple average of the LOS deformation rates of the different PS belonging to a single phenomenon is used as its representative velocity; this is done by analyzing separately historical and recent PSI data and calculating $V_{H,LOS}$ and $V_{P,LOS}$ for each mapped landslide. Nevertheless, depending of the specific landslide at hand, the use of the maximum value of observed PS velocities (peak velocity)—rather than their average—could be more suitable to describe the analyzed area; this approach follows the criteria suggested by Cruden and Varnes (1996), which promote the use of peak velocities of substantial portions of the displaced masses for the evaluation of landslide intensity.

Using simplified geomorphologic schemes, such as those proposed by Cascini et al. (2010), the conversion of LOS deformation values (V_{LOS}) to the most probable direction of displacement can be performed. For instance, assuming a pure translational mechanism, LOS velocities can be projected along the direction of the maximum slope, i.e., the steepest slope direction, obtaining $V_{H,SLOPE}$ and $V_{P,SLOPE}$ for the historical and present velocities, respectively (e.g., Greif and Vlcko 2011; Herrera et al. 2010). This step was applied for the test area of Verbicaro, as described in the following sections. Alternatively, if PSI data are available for both ascending and descending acquisition modes, the combination of these independent estimations along the two opposite geometries can be performed to better constrain the landslide movements; under the assumption of the absence of N–S horizontal motion, this combination may be used to reconstruct both the vertical and the E–W horizontal deformation components. Subsequently, the highest between these components can be used as the representative velocity for the analyzed phenomenon. Although the theoretical potentials of the combination of ascending and descending data are higher than those associated with the use of a single acquisition geometry, real practice shows significant difficulties in mountainous and hilly areas where the chances of retrieving radar targets in both geometries (ascending and descending) are significantly low due to geometrical visibility and distortions (see discussions).

When the distribution of PS deformation rates inside the landslide boundary is inhomogeneous (i.e., significantly variable PS velocities in the same landslide area), the estimation of a single representative rate for the whole phenomenon may be inappropriate; in those cases, a fragmentation or partition of the landslide area into two or more sectors with different deformation behaviors (and respective representative velocities) may also be performed. This can be done by tracing the boundaries between moving and stable parts of the same landslide mass and/or identifying portions characterized by significantly different deformation velocities (e.g., Greif and Vlcko 2011; Notti et al. 2010; Righini et al. 2011).

Activity matrices and intensity scales

Once the representative velocities of each landslide have been evaluated, PSI-based activity matrices and intensity scales are exploited to identify its state of activity and intensity (Fig. 1). Activity matrices and intensity scales are, respectively, 2D and 1D grids defined in terms of PS average annual velocity. They combine past and recent estimates of land deformation and may also include the information coming from the preexisting inventory map of the investigated area (Figs. 2 and 3). Such tools were used for the first time for medium scale applications by Righini et al. (2011) and Bianchini et al. (2012) and they are here standardized for a generic case study as well as improved through the consideration of the whole range of input data availabilities and combinations.

Activity and intensity thresholds

To build the activity matrices and intensity scales, two or more deformation thresholds have to be preliminarily fixed to discriminate moving/stable phenomena as well as different states of activity and intensities:

- V_{ACT}, distinguishing moving from nonmoving areas;
- V_{INT}, discriminating extremely from very slow landslides.

These values are strictly dependent on the case studies at hand and are empirically determined taking into account both the typology of deformation processes affecting the investigated area and the

Fig. 2 Activity matrix based on the exploitation of present $[D_{P1}-D_{P2}]$ PSI data and time-referenced information about the state of activity (e.g., preexisting inventory $[D_{INV}]$), usually employed for premapped landslides. V_{ACT} deformation threshold discriminating states of activity

Activity matrix for premapped landslides

Past time-referenced information about the state of activity are generally already available for those landslides identified through past investigations, such as phenomena included in preexisting inventory maps; date of reference of their activity estimation is here called D_{INV}. In these cases, a matrix combining this past evaluation with more recent PSI-derived estimates of ground displacements can, therefore, be employed to update or confirm the activity of these phenomena (Fig. 2). Input parameters of such a matrix thereby consist of:

– Time-referenced state of activity from a preexisting inventory, defined at date D_{INV};
– Representative velocity V_P, defined in the interval $[D_{P1}-D_{P2}]$, subsequent to D_{INV}.

The nine different combinations that constitute this first typology of activity matrix, and their outcomes in terms of updated activities and respective temporal references, can be summarized as follows:

1. Stabilized $[D_{INV}]$ landslides, whose V_P is:
    (a) Lower than V_{ACT} → Stabilized $[D_{P2}]$
    (b) Higher than (or equal to) V_{ACT} → Reactivated $[D_{P2}]$
    (c) Not assessable → Stabilized $[D_{INV}]$
2. Dormant $[D_{INV}]$ landslides, whose V_P is:
    (a) Lower than V_{ACT} → Stabilized/Dormant $[D_{P2}]$
    (b) Higher than (or equal to) V_{ACT} → Reactivated $[D_{P2}]$
    (c) Not assessable → Dormant $[D_{INV}]$
3. Active $[D_{INV}]$ landslides, whose V_P is:
    (a) Lower than V_{ACT} → Dormant/Active $[D_{P2}]$
    (b) Higher than (or equal to) V_{ACT} → Active $[D_{P2}]$
    (c) Not assessable → Active $[D_{INV}]$.

As pointed out by Bianchini et al. (2012), this typology of activity matrices are based on a 'conservative' or 'cautionary' approach; in other words, even if PSI data register low movement rates (i.e., V_P is lower than the chosen threshold, V_{ACT}), the state of activity recorded in the preexisting inventory cannot be lowered

specific characteristics of the available PSI data, e.g., landslide geometry, LOS direction, measurement precision, and relativity of PSI estimates with respect to the reference point. Examples of V_{ACT} velocity thresholds exploited for recent landslide studies at the regional scale range between ±1.5 and ±4.0 mm/year, referred to LOS data (Bianchini et al. 2012; Cascini et al. 2010; Farina et al. 2006; Meisina et al. 2006, 2008; Righini et al. 2011), whereas an example of LOS velocity threshold distinguishing extremely slow from very slow phenomena, V_{INT} is ±10 mm/year (Bianchini et al. 2012; Righini et al. 2011).

Criteria for choosing the different thresholds are tackled within the discussion and a simple operational methodology suggested for the selection of the thresholds is also experimented for the case study of Verbicaro which is analyzed as test area in the following section.

Fig. 3 Activity matrix based on the exploitation of historical $[D_{H1}-D_{H2}]$ and present $[D_{P1}-D_{P2}]$ PSI data, usually employed for new detections. Third column of **a** may be substituted with **b** to refer all the assessments to the date $[D_{P2}]$. V_{ACT} deformation threshold discriminating states of activity, NC not classified

(i.e., from dormant to stabilized, or from active to dormant), unless field evidences and in situ monitoring data confirm an actual lowering of activity (e.g., in Fig. 2, premapped dormant and active landslides showing recent PSI-derived velocity lower than V_{ACT}). This explains the ambiguous (double) classification of the combinations 2a and 3a within the above-mentioned list, which reflects the uncertainty in the assessment of the state of activity, resolvable only through field validation.

As observable from the above described matrix, the temporal coverage of PSI data influences the final time reference of the updated inventory; this will correspond to the last acquisition of the PSI monitoring interval. Thus, for those phenomena whose updating is performed by using PSI estimates, the reference will be $[D_{P_2}]$; for instance, the employment of Radarsat1 [2003–2009] data produces an updated inventory referenced to 2009. On the other hand, landslides with total absence or insufficiency of PSI-based deformation velocities (i.e., not assessable V_P) will retain the time reference of the inventory from which they belong to, i.e., $[D_{INV}]$. Causes and possible solutions to partial and total lack of PS within the landslide boundaries are tackled within the discussion.

Activity matrix for newly detected landslides

For newly detected landslides or those premapped phenomena lacking in past evaluation of activity, an activity matrix combining historical and recent deformation PSI data can be exploited. In this case, the input parameters of the matrix are:

– Historical representative velocity V_H, defined in the interval $[D_{H_1}–D_{H_2}]$;
– Present representative velocity V_P, defined in the interval $[D_{P_1}–D_{P_2}]$, subsequent to $[D_{H_1}–D_{H_2}]$.

The nine different combinations constituting this second type of activity matrix, and their respective outcomes, can be summarized as follows (Fig. 3a):

1. Landslides whose V_H is lower than V_{ACT} and whose V_P is:
    (a) Lower than V_{ACT} → Stabilized $[D_{P_2}]$
    (b) Higher than (or equal to) V_{ACT} → Reactivated $[D_{P_2}]$
    (c) Not assessable → Stabilized/Dormant $[D_{H_2}]$
2. Landslides whose V_H is higher than (or equal to) V_{ACT} and whose V_P is:
    (a) Lower than V_{ACT} → Dormant $[D_{P_2}]$
    (b) Higher than (or equal to) V_{ACT} → Active $[D_{P_2}]$
    (c) Not assessable → Active/Reactivated $[D_{H_2}]$
3. Landslides with not assessable V_H and whose V_P is:
    (a) Lower than V_{ACT} → Stabilized/Dormant $[D_{P_2}]$
    (b) Higher than (or equal to) V_{ACT} → Active/Reactivated $[D_{P_2}]$
    (c) Not assessable → not classified (NC).

Ambiguous classification of the combinations 1c, 2c, 3a, and 3b (Fig. 3a) are caused by the absence or insufficiency of PSI data for either the historical or the present monitoring interval; it reflects the uncertainty in the activity assessment due to the impossible comparison between movement conditions before and after a certain date (i.e., indiscernible history of deformation). As for the previous matrix, field checks and validation may clear up this uncertainty.

As well as for the first typology of matrices, the temporal coverage of PSI data also influences the time reference of the

evaluations for newly detected phenomena; for those phenomena whose updating is performed by using historical estimates, the reference will be $[D_{H_2}]$, while for present data it will be $[D_{P_2}]$. For instance, the employment of Envisat [2002–2010] data produces an updated inventory referenced to 2010, while the use of ERS1/2 [1992–2001] data references the updated phenomenon to 2001. In case of new phenomena lacking in both past and recent estimates, they will be attributed to the NC category (Fig. 3a).

An alternative for the matrix in Fig. 3a, is the substitution of its third column with the modified version which is shown in Fig. 3b and corresponds to the typology of matrix used by Righini et al. (2011). In this case, when the present PSI data are insufficient within the landslide boundary, but the information on the historical landslide velocity is available, conditions 1c and 2c are modified as follows:

1c) V_H lower than V_{ACT} → Stabilized/Reactivated $[D_{P_2}]$
2c) V_H higher than (or equal to) V_{ACT} → Dormant/Active $[D_{P_2}]$.

The difference with the original matrix in Fig. 3a consists in the reference time of the assessment of the state of activity. While in the original matrix the determination is considered ambiguous between the states of stabilized and reactivated at time $[D_{H_2}]$, in the modified version shown in Fig. 3b, the assessment of the activity is done at the reference time $[D_{P_2}]$ and the uncertainty is between the states of dormant and active continuous.

Intensity scale

The evaluation of landslide intensity is performed by comparing the PSI-derived landslide velocity not only with the activity threshold, V_{ACT}, but also with the intensity threshold, V_{INT}, which discriminates extremely from very slow velocities (Fig. 4). The only input parameter for the employment of this scale is the representative velocity of each landslide, in the present (or historical) interval, i.e., V_P (or V_H). The four different combinations constituting the intensity scale, and their outcomes in terms of intensities and respective temporal references, can, therefore, be summarized as follows:

1. V_P (or V_H) is lower than V_{ACT} → Negligible $[D_{P_2}]$ (or $[D_{H_2}]$)
2. V_P (or V_H) is higher than (or equal to) V_{ACT} but lower than V_{INT} → Extremely Slow $[D_{P_2}]$ (or $[D_{H_2}]$)
3. V_P (or V_H) is higher than (or equal to) V_{INT} → Very Slow $[D_{P_2}]$ (or $[D_{H_2}]$)
4. Neither V_P nor V_H are assessable → Not Classified (NC).

As for the activity matrices, the coverage of PSI data influences the time reference of the intensity evaluation, which will correspond to the last acquisition of the PSI monitoring interval, i.e., $[D_{P_2}]$ when using recent data or $[D_{H_2}]$ when using historical data. Total absence or insufficiency of PSI data induce the analyzed phenomenon to be attributed to the NC category (Fig. 4).

Test area of Verbicaro, Calabria (Italy)

A sheet pile of basement thrust units piled up and overthrust toward the Apulian foreland during the Neogene characterizes the geological background of the Calabrian peninsula in Southern Italy (Cucci and Cinti 1998). Hercinian crystalline and metamorphic basement units crop out; these are overlaid by Mesozoic and Tertiary sedimentary rocks, covered by Upper

Present (or historical) PSI data [D_{P1}-D_{P2}] (or [D_{H1}-D_{H2}])

	Sufficient n° and δ of PS		Insufficient n° or δ of PS
V_P (or V_H) < V_{ACT}	$V_{ACT} \leq V_P$ (or V_H)< V_{INT}	V_P (or V_H) ≥ V_{INT}	
NEGLIGIBLE [D_{P2}] or [D_{H2}]	**EXTREMELY SLOW** [D_{P2}] or [D_{H2}]	**VERY SLOW** [D_{P2}] or [D_{H2}]	**NC**

Fig. 4 Example of intensity scale based on the exploitation of present [D_{P1}–D_{P2}] or historical [D_{H1}–D_{H2}] PSI data. V_{ACT} deformation threshold discriminating states of activity, V_{INT} deformation thresholds discriminating intensities, *NC* not classified

Neogene and Quaternary sediments (Amodio Morelli et al. 1976). The whole peninsula shows mountainous and hilly morphologies and is highly susceptible to landslides due to high slope gradients, intense rainfalls, weathered and faulted crystalline-metamorphic rocks, and weakly consolidated sedimentary sequences. Associated with extensive human activities, such as urban sprawl and defor-estation, these factors contribute to production of steep and un-stable slopes (Carrara and Merenda 1976).

A small area in the province of Cosenza, in the northern sector of Calabria Region, was chosen as an example for the application of the PSI-based matrix approach: a sector extending ~14 km² and located within the municipality of Verbicaro. This choice was driven by the geomorphologic characteristics of this area and its assortment in terms of landslide activity and intensity as well as availability of PSI data for the different phenomena affecting its urban and suburban infrastructures.

The geological setting of Verbicaro is characterized by tecto-nostratigraphic units piled up and locally dislocated by normal faults. The Alpine basement assemblage, previously deformed, structurally overlies the Appennine carbonate succession and its Paleogene-Lower Miocene cover (Van Dijk et al. 2000; Ferranti et al. 2009). The outcropping lower unit is made of a thick Triassic dolomite interval and a Jurassic cherty limestone succession of variable thickness (Iannace et al. 2005). Dolomites and well-strat-ified limestones are in stratigraphic continuity and derive from the Mesozoic carbonate platform; this unit represents a deformed complessively 4,000-m thick sequence, which now forms the back-bone of the Pollino Range (Cucci and Cinti 1998) and outcrops eastward within the area of interest (Fig. 5). Mesozoic limestones sometimes include basic volcanic elements. The carbonate succes-sion is covered, in disconformity, by a Paleocene-Lower Miocene open shelf turbiditic calcarenites and coarse calcareous breccias. The upper element is composed of alpine metasedimentary rocks that mostly comprise schistes, fillads, and calceschistes (Scisti del Fiume Lao Formation); these deep basinal metapelitic rocks highly tectonized, outcrop throughout the investigated area and have been included in the ophiolite-bearing Frido Unit of the Calabrian borderland, overlying platform carbonates (Ferranti et al. 2009; Iannace et al. 2005; Van Dijk et al. 2000). Upper Pliocene-Pleistocene undisturbed terrigenous deposits fill the area, covered by recent Quaternary continental deposits (Cucci and Cinti 1998). Outcropping terrains are sliced by Quaternary high-angle strike-slip and extensional faults (Ferranti et al. 2009) that cut the ridges of the test area westward into fault-bounded blocks.
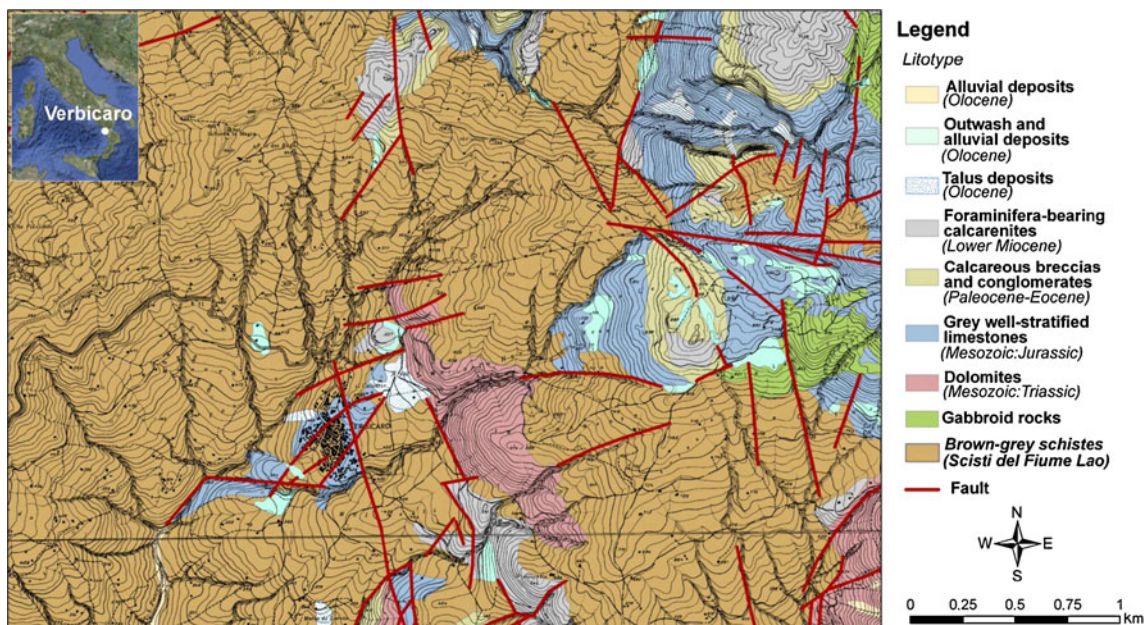

Fig. 5 Geological setting (modified from geological map 1:25,000, Regional Cartographical Centre, 1969) and geographic location (*inset*) of Verbicaro, Northern Calabria (Italy), overlapped on a 1:10,000 topographic map

The preexisting inventories available for the test area are the Hydrogeological Setting Plan (Piano Stralcio per l'Assetto Idrogeologico, PAI) produced by the River Basin Authority of Calabria Region in 2001 with following modifications until 2006 and the Italian Landslide Inventory (Inventario Fenomeni Franosi in Italia, IFFI) produced by the Italian Institute for Environmental Protection and Research in 2007. Both PAI and IFFI inventories were created on a reference scale of 1:10,000 and employed aerial photointerpretation, field campaigns, and local databases. IFFI was compiled updating the PAI inventory; hence, it includes all the information of the PAI and was thereby used as the primary map to be analyzed for Verbicaro. Inside this inventory, three different states of activity are distinguished, i.e., active (including active, reactivated, and suspended), dormant, and stabilized (including artificially and naturally stabilized).

The municipality of Verbicaro has been classified by the PAI as a municipality affected by very high hydrogeological risk, determined on the basis of the effects on settlement, manufactures, and population, as defined by the Italian Decree Law no. 180/98 concerning urgent measures for risk prevention; the PAI zonation also estimates the extent of the high and very high risk areas of the municipality—whose total extent is ~32.6 km²—as exceeding 0.15 km², thus collocating the municipality in the highest risk class. The whole municipality is characterized by a mountainous morphology with dense network of narrow rivers and waterways and is affected by several large landslides, especially in the urban and suburban areas of the main village, which were selected as test sites for the application of the PSI-based matrix approach. The last important activation of some of these phenomena dates back to February 2010 when the provincial road, which guarantees the main access to the village, was partially buried by debris moved downhill from the overlying slope.

Within the area selected as test site, a total of 24 landslides are mapped in the preexisting inventory of IFFI. For the sake of simplicity and to identify them easily, we have assigned these unstable areas a short code, going from L1 to L24 (Fig. 6 and Table 1). Most of the identified phenomena are classified as rotational/translational slides (i.e., L6 to L13, and L16 to L21) and complex movements (i.e., L1 to L5, and L22 to L24), and involve mainly low-grade metamorphic rocks and occasionally well-stratified limestones. A dormant complex landslide, L22, constitutes the larger phenomenon affecting the area, with an extension of ~2.1 km². It involves the whole northwestern sector of the village of Verbicaro and is partially overlaid by smaller-scale active slides and complex landslides (e.g., L5 to L7) as well as a flowlike phenomenon characterized by N to S motion direction (L15) and, to the S, a complex landslide (L1) whose foot reaches the village downstream. The larger portion of Verbicaro village is affected by phenomena moving towards W and SW, mainly complex (L2 to L4) and rotational/translational slides (e.g., L10, L11, L17, and L18). The latter overlay a dormant complex landslide (L24) involving the whole left bank of the incision where L1 flows. Despite limited extension of these phenomena, generally less than 0.07 km², they represent a major cause of risk for local population and urban structures, since their main bodies involve the whole portion of the village located on the W and SW facing slopes. Only small portions of the village are excluded from the unstable zones identified by the PAI and IFFI inventories, such as the elongated zone between phenomena L4 and L18 and that between L2 and L14; however, the geomorphologic indicators and the proximity to active landslides suggest potential enlargement of the landslide boundaries to include also some sectors of the urban area, as described in the following sections.

Application of the PSI-based matrix approach

Input data
For the implementation of the PSI-based matrix approach to the area of Verbicaro, the IFFI inventory was used as the primary map
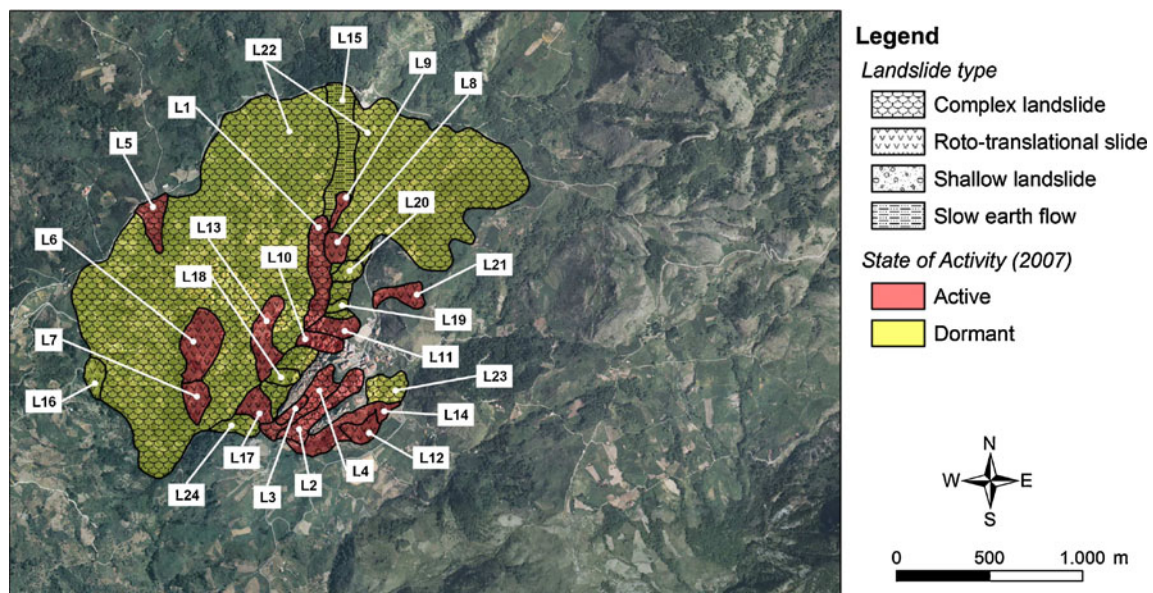

Fig. 6 Preexisting landslide mapping in the area of Verbicaro, overlapped on a color orthophoto acquired in 2000

Table 1 Summary and statistics of the PSI-based assessment of landslide states of activity and intensity in the area of Verbicaro, Italy, with respective reference years. α azimuth, β slope, A active, R reactivated, D dormant, S stabilized, N negligible, ES extremely slow, VS very slow, NC not classified, – absence of PS

ID	Preexisting information [2007]					ERS1/2 [1992–2000]		RSAT1 [2003–2010] and RSAT2 [2009–2011]			Updated inventory	
	Area (km^2)	Type	Activity	α (°)	β (°)	$V_{H,LOS}$ (mm/year)	$V_{H,SLOPE}$ (mm/year)	$V_{RSAT1,LOS}$ (mm/year)	$V_{RSAT2,LOS}$ (mm/year)	$V_{P,SLOPE}$ (mm/year)	Activity [year]	Intensity [year]
L1	0.056	Complex landslide	A	174	13.9	0.1	1.3	−0.2	−1.0	18.0	A [2011]	VS [2011]
L2	0.062	Complex landslide	A	227	12.8	–	–	−19.2	−20.0	38.8	A [2011]	VS [2011]
L3	0.009	Complex landslide	A	242	14.0	−16.6^a	31.9^a	–	−19.0^a	30.2^a	A [2007]	NC
L4	0.050	Complex landslide	A	216	14.1	−18.4	48.2	−19.9	−20.9	47.4	A [2011]	VS [2011]
L5	0.029	Complex landslide	A	202	14.6	–	–	–	–	–	A [2007]	NC
L6	0.064	Rototranslational slide	A	202	13.7	–	–	−10.5^a	−11.1^a	36.1^a	A [2007]	NC
L7	0.025	Rototranslational slide	A	210	15.9	–	–	–	–	–	A [2007]	NC
L8	0.019	Rototranslational slide	A	170	16.1	–	–	–	–	–	A [2007]	NC
L9	0.010	Rototranslational slide	A	194	14.9	–	–	–	−0.2^a	0.8^a	A [2007]	NC
L10	0.03	Rototranslational slide	A	255	15.0	−16.1	27.7	−19.9	−21.9	31.2	A [2011]	VS [2011]
L11	0.069	Rototranslational slide	A	251	21.2	−9.7	14.8	−16.0	−14.5	21.4	A [2010]	VS [2010]
L12	0.020	Rototranslational slide	A	254	10.8	–	–	–	–	–	A [2007]	NC
L13	0.049	Rototranslational slide	A	182	15.0	−9.6	55.5	−9.0	−9.8	77.2	A [2010]	VS [2010]
L14	0.057	Shallow landslide	A	239	11.8	−7.6	16.1	−14.1	−12.0	24.7	A [2010]	VS [2010]
L15	0.079	Slow Earth flow	D	212	16.6	–	–	−1.0^a	−0.4^a	2.4^a	D [2007]	NC
L16	0.019	Rototranslational slide	D	178	18.4	–	–	–	–	–	D [2007]	NC
L17	0.025	Rototranslational slide	A	257	18.0	−10.2^a	16.2^a	–	−17.0^a	22.7^a	A [2007]	NC
L18	0.014	Rototranslational slide	D	277	20.0	−13.7^a	20.0^a	−16.3	−17.3^a	20.7	R [2010]	VS [2010]
L19	0.007	Rototranslational slide	D	264	16.9	−22.0^a	34.9^a	–	−30.5^a	40.4^a	D [2007]	NC
L20	0.015	Rototranslational slide	D	275	18.9	−14.9^a	22.3^a	−3.2	−7.0	8.7	R [2011]	ES [2011]
L21	0.034	Rototranslational slide	A	243	23.2	−4.6	7.0	−1.5	−13.0	17.6	A [2011]	VS [2011]
L22	2.107	Complex landslide	D	181	15.5	−5.4	30.7	−10.3	−6.8	89.2	R [2010]	VS [2010]
L23	0.031	Complex landslide	D	216	16.3	−1.0	2.5	−1.5	−1.3	3.3	D/S [2010]	N [2010]
L24	0.107	Complex landslide	D	267	16.9	−16.5	25.9	−18.6	−19.8	26.0	R [2011]	VS [2011]
L25	New detection			233	18.2	−6.8	12.8	−8.1	−9.9	16.0	A [2011]	VS [2011]
L26	New detection			256	13.1	−11.6	20.8	−16.7	−12.1	24.5	A [2010]	VS [2010]

^{a} Less than 4 PS within the landslide boundary (unreliable estimation)

to be updated, setting the D_{INV} as 2007, corresponding to the reference year of this inventory. As for the PSI data, the following three sets were employed (Fig. 6):

- ERS1/2 stack consisting of 78 scenes in descending mode, spanning the interval 17/05/1992–20/12/2000, VV polarization, look angle 23.4 °, and directional cosines: 0.38972 (E), −0.07976 (N), 0.91747 (Z).
- Radarsat1 Standard Beam S3 stack consisting of 80 scenes in descending mode, spanning the interval 19/03/2003–17/01/2010, HH polarization, look angle 34.5 °, and directional cosines: 0.55423851 (E), −0.11857239 (N), 0.82386907 (Z).
- Radarsat2 Standard Beam S3 stack consisting of 33 scenes in descending mode, spanning the interval 10/01/2009–06/04/2011, HH polarization, look angle 33.9 °, and directional cosines: 0.54939554 (E), −0.09516750 (N) and 0.83012510 (Z).

D_{H1} and D_{H2} were thereby set to 1992 and 2000, while D_{P1} and D_{P2} corresponded to 2003 and 2010 for the Radarsat1 stack, and 2009 and 2011 for the Radarsat2 stack.

Although the use of both ascending and descending data stacks is generally suggested to implement the approach, for Verbicaro, only data stacks with descending acquisition geometry were used. This is due to the local morphology of the area which is predominantly oriented in the SW, W, and NW directions and consequently prone to be analyzed with PSI descending data.

Historical ERS1/2 data were processed with the PSInSAR (Permanent Scatterers Interferometric SAR) technique by TRE S.r.l. (Ferretti et al. 2001) in the framework of the Piano Straordinario di Telerilevamento Ambientale (PST-A) project, while Radarsat1 and Radarsat2 stacks were processed—into two separate stacks—by e-GEOS with the Persistent Scatterers Pairs (PSP) technique (Costantini et al. 2000) in the framework of the European project Services and Applications for Emergency Response (SAFER). The resulting stacks of radar targets are characterized by similar spatial distribution and density, even given the different approaches employed for the processing of the available stacks, i.e., the Persistent Scatterers concept, used by the PSInSAR technique, and interferogram stacking concept, used by the PSP. Higher density of targets is retrieved for build-up sectors of Verbicaro and exposed rocks characterizing the eastern portion of the test area, while the densely vegetated zones prevented stable scatterers to be identified (Fig. 7). Reference points of each PS stack (zero deformation points) were selected, taking into account not only the phase stability of the PS candidates analyzed during the processing but also the geological setting of these coherent points and verifying the absence of local-scale motions affecting the areas selected as reference. In particular, three different locations over postorogene Plio-Pleistocene deposits, between 30 and 60 km E of the area of Verbicaro, were selected; the distance of the three reference points from Verbicaro and the choice of three different locations are due to the PSI data belonging to stacks of imagery with slightly dissimilar spatial coverage (extension of the processing area) and different coherence variations in time and space.

PS velocities showed higher variability in space for the Radarsat2 stack in the whole area of Verbicaro (Fig. 7c). This is justified by the lower number of scenes used to perform the PSP processing, the short temporal interval (only 2 years) and significant orbital and atmospheric errors, and the consequent lower precision in the

estimated velocities. Standard deviations of Radarsat2 targets ranged between 1.1 and 4.1 mm/year, unlike the lower values recorded for the other two stacks, i.e., 0.6–1.0 mm/year for Radarsat1 and 0.4–0.8 mm/year for ERS1/2.

Preparatory phase

The ancillary data used to support photo and radar interpretation included topographic maps at scales 1:10,000 (produced in the 1950s by the Regional Cartographic Center) and 1:25,000 (1990s; Italian Military Geographic Institute), a geological map at 1:25,000 (1960s; Regional Cartographic Center), a Digital Terrain Model (DTM) with 20-m resolution and its derived maps (1990s; Italian Military Geographic Institute), and colored aerial orthophotos with 1-m resolution (1998–1999). The preexisting inventory of the IFFI project was first updated and improved combining a monoscopic photo interpretation of the aerial orthophotos with the radar interpretation of PSI-derived ground motion data in 1992–2000 (ERS1/2 descending) and 2003–2011 (Radarsat1 and Radarsat2 descending). The methodology employed to update the boundaries of premapped phenomena and to identify new landslides followed the approach of LHSM described by Bianchini et al. (2012). Orthophotos, DTM, and derived layers (aspect, slope, and hillshade) facilitated the identification of landslides in the vegetated areas outside the Verbicaro village, while PSI data were mostly used to update the landslide boundaries within the built-up areas. For eight premapped landslides, we applied modification to their boundaries (Fig. 8); an example is the enlargement of the boundary of L11 in the E direction to include the clearly recognizable head, minor and major scarps (Fig. 9), or the extension of L2 to the NNE direction to include a nonpreviously mapped portion of the urban area.

Two additional phenomena, L25 and L26, were also detected by exploiting the information gathered from optical and radar data; both can likely be attributed to the typology of complex movements. L25 affects the eastern sector of the test area and involves a sparsely vegetated SW-facing slope less than 1 km far from the village of Verbicaro and characterized by weathered bare rocks made of well-stratified limestones, calcareous breccias, and conglomerates, partially covered by alluvional deposits. Several blocks of sizes variable between few cubic centimeters and decimeters can be observed in this area (Fig. 10). Their movement is attributable to the typologies of falls, topples or slides, depending on local factors such as the geometrical proportions of each block (height to width ratio) and the slope inclination. A significant amount of PS in all the three available stacks was retrieved within the boundary of L25: 200 ERS1/2, 420 Radarsat1, and 540 Radarsat2 targets. We observe similar spatial distributions of LOS velocities within the landslide, with higher values concentrated in the foot (up to −21.3 mm/year in 2009–2011) where the slope is steeper (up to 40 °) and thus closer to the LOS geometry; lower rates (−5 to −10 mm/year in all the time intervals) are observed in the main body where the morphology is gentler. L26 involves a more densely vegetated WSW-facing slope in the southwestern portion of the suburban area of Verbicaro, which lies on metamorphic rocks and, in its northern portion, limestones. Its morphology is gentler than that of L25, with slopes averagely 13 °, but never exceeding 25 °. The presence of vegetation here hampers the identification of PS and induces the three data stacks to be populated by less than 80 PS in total. Velocities are higher in the northern portion of the landslide
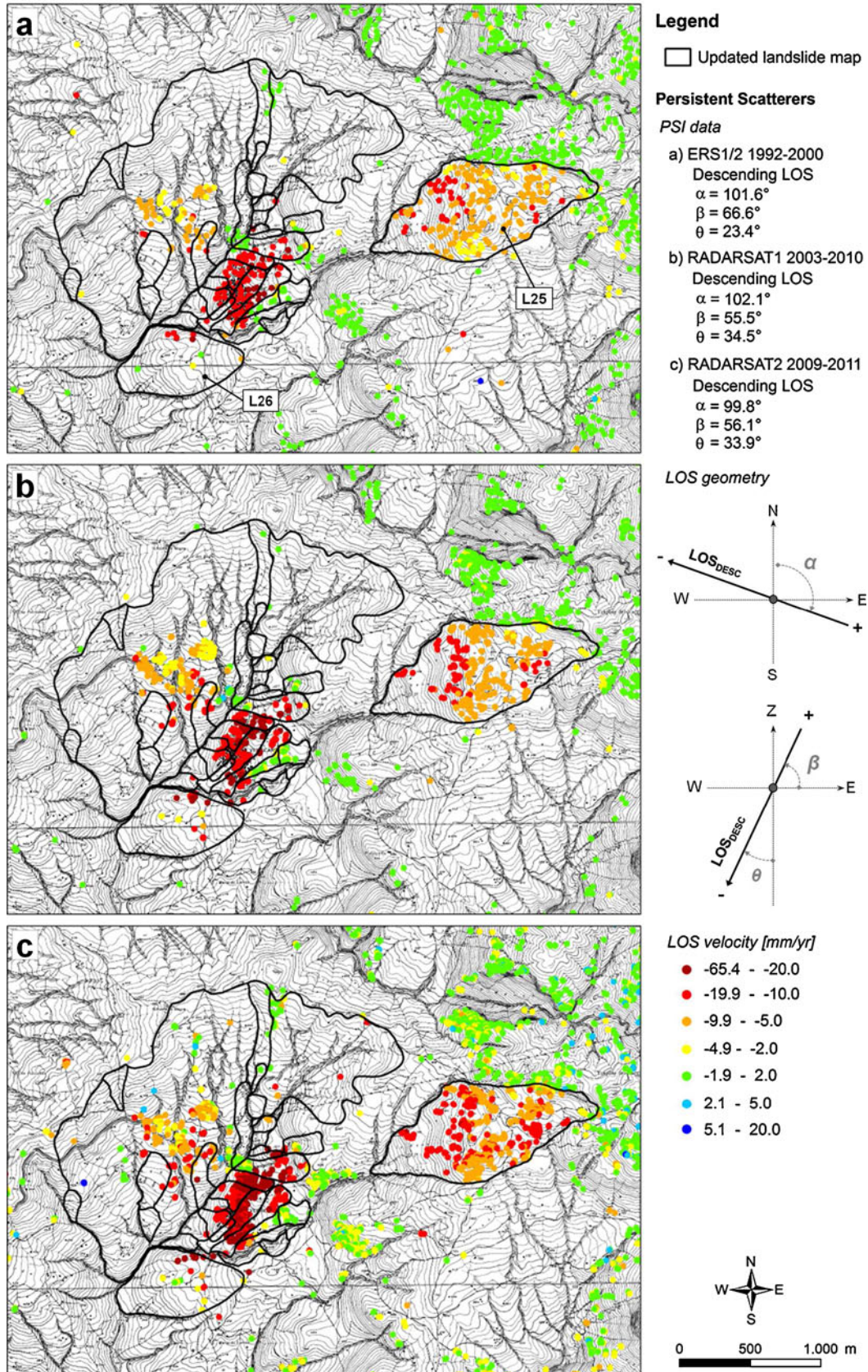
Fig. 7 Updated landslide inventory and PSI-derived deformation in 1992–2001 (**a**): ERS1/2 data, descending), 2003–2010 (**b**): RADARSAT1 data, Standard Beam mode S3, descending), and 2009–2011 (**c**): RADARSAT2 data, Standard Beam mode S3, descending) in the area of Verbicaro, overlapped on a 1:10,000 topographic map

Fig. 8 3D view of the updated landslide mapping in the Verbicaro village, captured from SW at ~45 ° angle. Heights of the DEM are amplified by a factor of 1.3. Direction of landslide movements and main modifications to the preexisting inventory are also shown
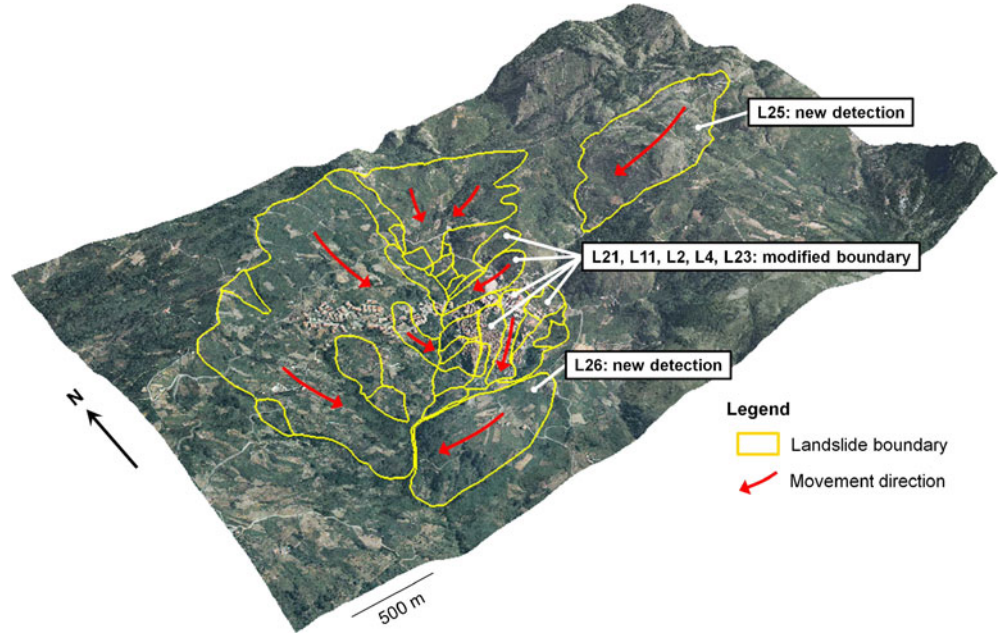
body where the orientation of the slope is closer to the descending LOS geometry and reach no more than 25–30 mm/year in the direction away from the sensors in all the available stacks.

In some other sectors of the test area, moving PS were not considered as part of nonmapped landslides because geomorphologic and geological evidences did not show actual presence of landslide processes. Moreover, some single unstable targets of the ERS1/2 and Radarsat1 stacks were attributable to settlements of single structures and not indicative of landslide occurrences.

Implementation

The representative velocities of the 26 landslides (L1 to L26) in the historical ($V_{H,LOS}$) and present ($V_{P,LOS}$) intervals were evaluated as the average yearly velocity of the available ERS1/2 and Radarsat1/2 PS data included within each landslide area. Given the availability of two different stacks of recent PSI data (Radarsat1 and Radarsat2) and considering their slightly different acquisition geometries, we preliminarily assigned two different representative velocities to each landslide, $V_{RSAT1,LOS}$ [2003–2010] and $V_{RSAT2,LOS}$ [2009–2011]. For both historical and recent PSI data, the calculation of the representative velocities was performed only for those unstable areas where a sufficient number of PS data was retrieved (at least 4 PS within the landslide boundary).

Using a simplified geomorphologic scheme, we assumed the motions affecting the area to be purely translational mechanisms; thus, we converted LOS deformation data in the descending mode (V_{LOS}) to the most probable direction of displacement, i.e., the direction of the maximum slope (steepest slope direction). The conversion to slope velocity (V_{SLOPE}) was performed—for each landslide—using the equations:

$$V_{SLOPE} = \rho_{L2S} \cdot V_{LOS} \qquad (1)$$

$$\rho_{L2S} = (E_{LOS} \cdot E_{SLOPE} + N_{LOS} \cdot N_{SLOPE} + Z_{LOS} \cdot Z_{SLOPE})^{-1} \qquad (2)$$

where the value ρ_{L2S} represents the conversion factor of LOS to SLOPE values, and E, N, and Z are the directional cosines of the LOS and the SLOPE vectors in the east, north, and zenith directions respectively.

The azimuth (α) and slope (β) angles of the steepest slope direction (SLOPE) were evaluated, respectively, as the average of the aspects and slopes of the DTM cells included within the updated landslide boundaries (Table 1) and then
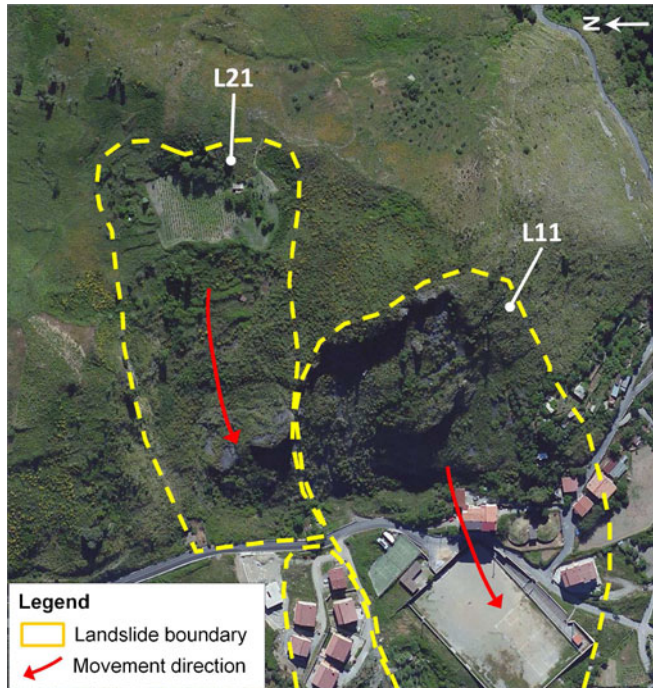

Fig. 9 Aerial view of landslides L21 and L11after the updating of their boundaries through photo- and radar interpretation (modified from Bing Maps© Microsoft)

used to estimate the directional cosines of the SLOPE, employing the formulas:

$$E_i = sin\alpha_i \cdot cos\beta_i \tag{3}$$

$$N_i = cos\alpha_i \cdot cos\beta_i \tag{4}$$

$$Z_i = sin\beta_i \tag{5}$$

Considering the cell resolution of both the ERS1/2 and Radarsat1/2 imagery (i.e., 20–30 m on the ground), the spatial resolution of the employed DTM (20 m) was considered appropriate for this calculation.

For the implementation of the matrix approach, we used the ERS1/2-based velocity estimate as the historical representative velocity ($V_{H,SLOPE}$), while as the present velocity ($V_{P,SLOPE}$), the highest between $v_{RSAT1,SLOPE}$ and $v_{RSAT2,\,SLOPE}$ and the respective reference year [D_{P_2}] (i.e., 2010 or 2011) was prudentially selected. Given the standard deviations of the three sets of PSI data available for Verbicaro (mentioned above), the LOS value of ±2 mm/year can be generally considered as an appropriate threshold discriminating moving from nonmoving targets (green PS in Fig. 6). The activity threshold V_{ACT} is set by taking into account the average reprojection factor (ρ_{LS}) of all the landslides mapped in Verbicaro with respect to the three descending LOS of ERS1/2, Radarsat1, and Radarsat2. This average factor has the value of 2.5 for Verbicaro; it means that, for this area, the LOS directions are able to detect approximately 40 % of slope-oriented displacements; hence, an increment of 150 % is needed to convert LOS to SLOPE estimates. The V_{ACT} to be applied to the SLOPE-projected velocities was thereby set as ±5 mm/year.

V_{INT} of ±13 mm/year was selected to discriminate extremely slow from very slow phenomena; the official threshold of 16 mm/year (Cruden and Varnes 1996) was precautionarily reduced by ~20 % to account not only for the difference between peak values and temporally averaged velocities (PSI-derived estimates are averages over long observation periods) but also for the spatial averaging that was performed to assess the representative velocity of each analyzed phenomenon. The application of identical thresholds for both ERS1/2 and Radarsat1/2 data do not represent major source of errors in the present application, since LOS velocities of all the PSI stacks were preliminarily reprojected along the slope directions and so cannot be considered influenced by the slightly different orientations of the employed LOS.

Results

Active complex landslides, L1 and L4, and rototranslational slides, L10, L11, L13, L14, and L21, showed sufficient number of both historical and present PS data within their boundaries (Table 1, Fig. 11). According to the activity matrix shown in Fig. 2, specifically devoted to premapped phenomena, only the present representative velocities were considered for the application of the PSI-based matrix approach. All these landslides revealed $V_{P,SLOPE}$ exceeding the activity threshold of ±5 mm/year and were thereby reattributed to the state of active (A), with new reference year of 2011 (L1 to L4, L21) or 2010 (L11, L13, L14)—depending on the Radarsat stack showing the highest rates. Similar to these phenomena, L22 to L24, previously classified as dormant complex landslides, were updated using the matrix of Fig. 2; in particular,

while for L22 and L24, the $V_{P,SLOPE}$ exceeded the activity threshold and induced them to be classified as reactivated (R), for L23 we observed a representative velocity lower than the threshold suggesting the stabilization of this phenomenon. However, following the conservative principle of not lowering the activity before confirming the actual lowering through on-site validation, we attributed to L23 the ambiguous state of dormant/stabilized (D/S). As for the assessment of the intensity of these premapped phenomena, all were classified as very slow (VS), since their $V_{P,SLOPE}$ were all higher than the intensity threshold of ±13 mm/year (Fig. 4); an exception was the L23 which was attributed to the class of negligible (N), since its velocity $V_{P,SLOPE}$ was of only a few millimeters per year (Table 1).

Complex landslide, L2, active in 2007, and rototranslational slides, L18 and L20, dormant in 2007, showed typical situations occurring when one or more stacks of PSI data are not available or insufficiently distributed within the landslide boundaries. For L2 and L20, PSI-derived estimates of ground deformation were only available (or reliable) for the present scenario (i.e., Radarsat1/2 stacks; Fig. 11b). In this particular case, given that these phenomena belong to the premapped landslides and that the use of historical PSI data is unnecessary (Fig. 2), no difference in the application of the methodology was applied with respect to the previously described cases: for L2, the active (A) state was confirmed and the very slow intensity (VS) was attributed, given that its $V_{P,SLOPE}$ exceeded both the V_{ACT} and the V_{INT}. On the other hand, for L20, the state of activity was updated to reactivated (R) and the intensity to extremely slow (ES) in 2011, as its $V_{P,SLOPE}$ was between V_{ACT} and V_{INT} (Figs. 4 and 11). Phenomenon L18 showed a particular scenario where only one of the present stacks of PSI-derived estimates is available, in particular, the Radarsat1 one; Radarsat2 PS were less than four within the landslide boundary, hence considered not reliable for the methodology. In this case, the implementation of the matrix approach was done using the Radarsat stack of estimates in the period 2003–2010, and this conditioned the reference year of the updating which was set to 2010 (Table 1). For all the other premapped landslides (i.e., L3, L5 to L9, L12, L15 to L17, and L19), partial lack or total absence of PSI data was observed within the respective boundaries and thereby the employment of the matrix of Fig. 2 and the scale of Fig. 4 caused these phenomena neither to be updated in terms of state of activity (their reference year was left as 2007) nor to be attributed an intensity (NC phenomena; Fig. 11c and d).

Summing up, for 13 of the 24 premapped landslides, the activity was updated to 2011 or 2010 and the intensity was also assessed with same reference year; on the other hand, for the remaining 11 phenomena, the activity recorded in the IFFI inventory was left unchanged and no evaluation of the intensity was performed due to the absence or insufficiency of PS data within the boundaries of these landslides (NC). A total of four reactivated (R), 16 active (A), three dormant (D), and one dormant/stabilized (D/S) phenomena were finally identified. Considering the intensity, the 13 updated landslides were distributed as follows: 11 very slow (VS), one extremely slow (ES), and one negligible (N).

The two newly identified phenomena, L25 and L26, were covered by PSI data in all the available stacks, i.e., ERS1/2, Radarsat1, and Radarsat2 (Table 1). Both these unstable areas showed historical and present velocities exceeding the activity threshold of ±5 mm/year and the intensity threshold of ±13 mm/year. L25 average motions in the slope direction were 12.8 and 16.0 mm/year in 1992–2000 and 2009–2011 respectively, while L26 showed slightly higher rates, i.e., 20.8 and 24.5 mm/year in 1992–2000 and 2003–2010. These

Fig. 10 3D view of landslide L25 (**a**) and two Street Views (© Google) captured in 2011 within its boundaries, (**b**) and (**c**)
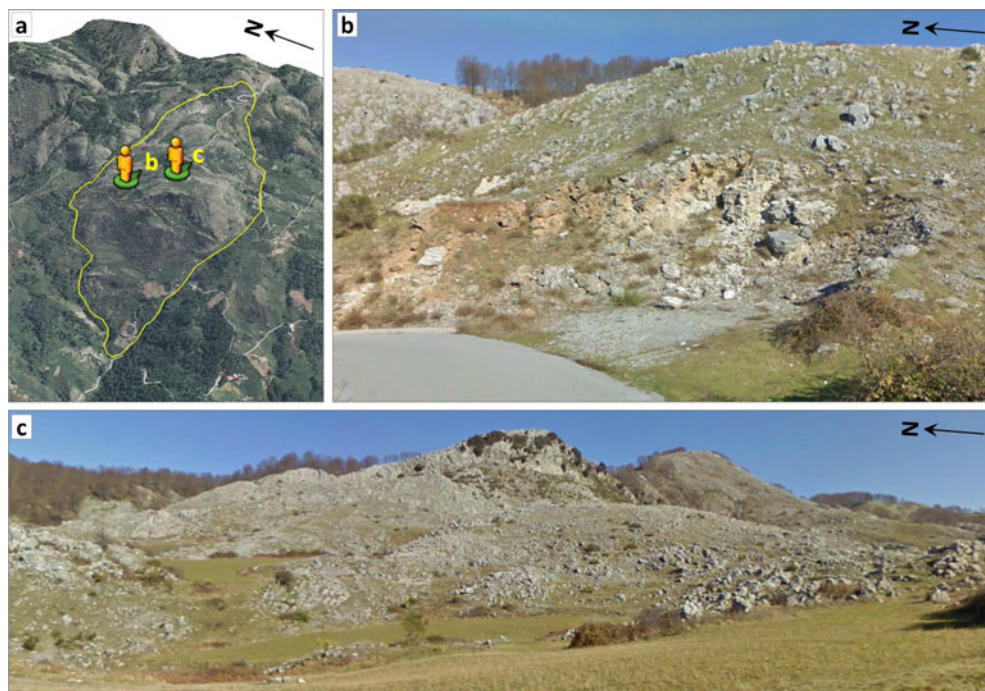
phenomena were thereby attributed the state of active (*A*) and the intensity of very slow (VS); L25 had a new reference year of 2011 and L26, with year 2010 (Fig. 11).

Given the areal extension of L25 and the variable morphology of this unstable area (Fig. 10), the use of a unique representative velocity for the whole phenomenon can be considered inappropriate. Further
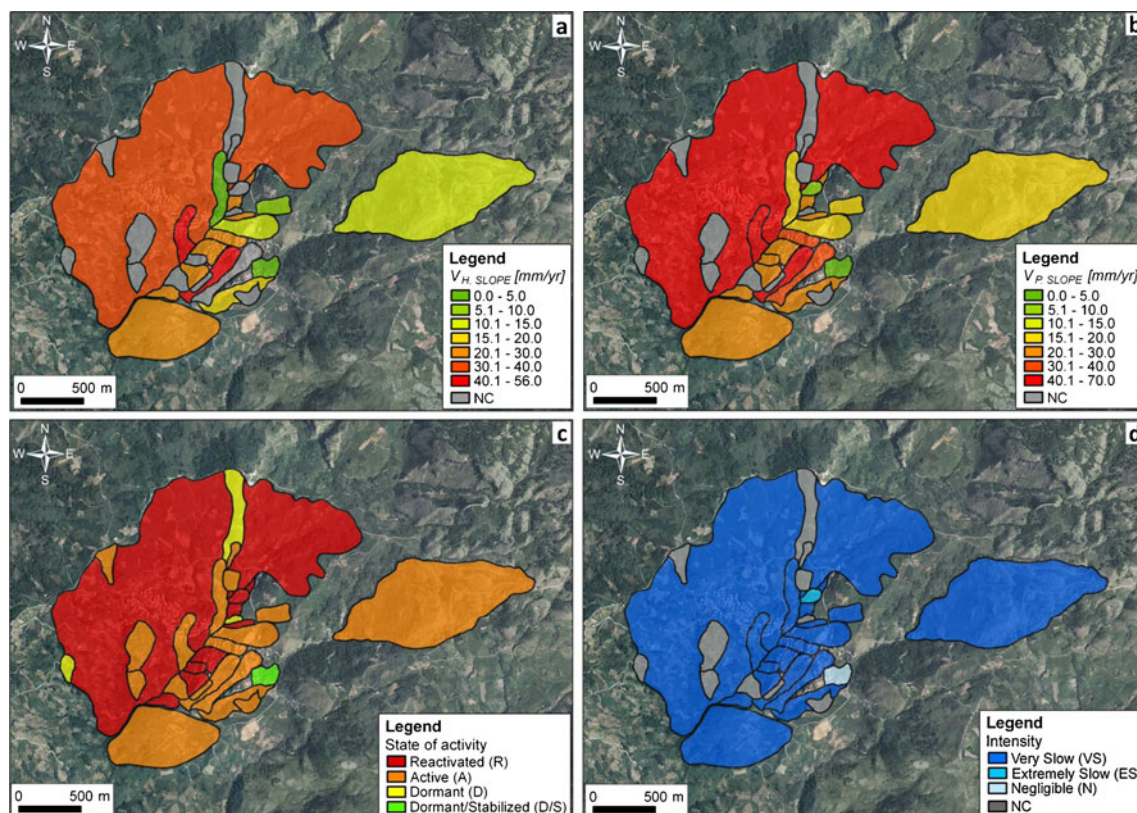

Fig. 11 Historical (**a**) and present (**b**) representative velocities, and states of activity (**c**) and intensity (**d**) of landslides mapped in Verbicaro, overlaid on a color orthophoto. Summary and statistics of PSI-derived data and main modifications to the preexisting landslide inventory are shown in Table 1

studies could be focused on a segmentation of the unstable area into subsectors of homogeneous morphology for which sector-specific velocities might be calculated. Alternatively, a cell-by-cell projection of PS LOS velocities along the slope direction of each DTM cell might be performed to account for the local differences in the morphology of this unstable area. Considering the scope of this work and the scale of application of the PSI-based matrix approach (generally, regional), these further steps are not tackled in this paper but postponed to future experimentations.

Discussion

Major influencing factors of the PSI-based matrix approach, its current limitations, and their respective solutions emerged through both the application to the test area of Verbicaro and the previously cited PSI-based landslide investigations, and can be summarized as follows.

Partial or total lack of PS within the landslide boundary

Total lack or insufficiency of targets within the landslide boundaries induce uncertainties in the activity and intensity evaluations, or even prevent the analyzed phenomena to be classified and/or updated (e.g., landslides L5 to L9 in Verbicaro). The different factors that influence the identification of radar targets during a PSI analysis are as follows.

Geometrical visibility

Combination of local topography and LOS orientation may cause significant underestimation of land motions, or even hamper the identification of PS within the observed scene, due to foreshortening, layover, and shadowing effects (Colesanti and Wasowski 2006). The geometrical visibility of a slope depends on its aspect and inclination (with respect to the sensor acquisition geometry, i.e., the LOS orientation) and can also vary within different portions of the same landslide (see, Cascini et al. 2010). Use of appropriate geometry for the investigated area is, therefore, fundamental for each PSI-based analysis. Generally, ascending acquisition modes are suitable for E-facing slopes where the landslide movements are likely to be oriented in the E direction, while descending modes are used for W-facing slopes. Availability of both ascending and descending data obviously increases the number of the areas investigable through PSI data. Different look angles of available SAR sensors and the flexibility of some satellites to vary their acquisition geometry (e.g., Radarsat and TerraSAR-X) need also to be taken into account while planning a PSI investigation.

A feasibility analysis of the geometrical visibility and target density that can be achieved through a PSI analysis for a given area of interest can be performed by exploiting one of the different criteria developed in the last years. Colombo et al. (2007) forecast the PS density of an area by cross-combining the effects of radar geometry (i.e., layover and shadowing), local topography (i.e., slope and aspect) and land use; Notti et al. (2010) summarize the previous visibility factors introducing the RC-index; Cascini et al. (2010) discuss and implement the approach of a priori DInSAR landslide visibility mapping.

Vegetation

Complementarily to the exploitation of optical photointerpretation, landslides observable with radar interpretation are concentrated primarily in urbanized/built-up areas. Vegetation cover causes temporal decorrelation and makes difficult the identification of stable radar targets. Deeper penetration of vegetation may be achieved using higher radar wavelengths, such as those of the L band (e.g., 23 cm for ALOS PALSAR data).

Use of corner reflectors may improve the density of monitored targets in semivegetated, agricultural, and also urban areas by installing on the ground artificial benchmarks which act as PS (e.g., planar, dihedral, and trihedral reflectors; Savio et al. 2005); however, this solution cannot overcome the lack of targets in archived SAR scenes clearly because the identification of corner reflectors is achieved only after their installation on the ground.

Rapid movements

Intensity classes higher than 'very slow' cannot be considered yet in the PSI-based matrix approach. This is due to the acquisition parameters and characteristics of the currently available SAR sensors that do not enable the estimation of deformations faster than few tens of centimeters per year, which would compromise the results of the PSI processing. Aliasing effects, due to the ambiguous nature of the 2π wrapping of interferometric phases, limit to a quarter of the wavelength the maximum displacement between two successive acquisitions and two close PS of the same dataset (e.g., Hanssen 2005; Crosetto et al. 2010). Velocities compromising the PSI processing depend on the employed SAR wavelengths and satellite revisiting times; they are about 15 cm/year for ERS/Envisat data (C band), 20 cm/year for Radarsat (C band), 25 cm/year for TerraSAR-X (X band), and 45 cm/year for ALOS/JERS (L band). Consequently, higher motion rates cannot be tracked and/or interpreted correctly. Future improvements of the PSI-based approach could be achieved by exploiting future SAR missions employing higher temporal frequencies, or even conventional InSAR (single interferograms) or Ground-Based InSAR (GBInSAR; e.g., Antonello et al. 2004) techniques, which can extend the velocity range of applicability of the matrix approach to include faster phenomena.

Temporal coverage of PSI data

Modification of temporal scale for activity assessment

Depending on the temporal coverage of PSI-derived deformation data, the matrix approach may modify the temporal scale for the evaluation of the states of activity, changing the time interval for discriminating different states from a single cycle of seasons (i.e., 12 months; WP/WLI 1993) to two or more years (e.g., 2 years, using 2009–2011 Radarsat2 data for the analysis of recent deformation velocities in Verbicaro). The lengthening of the reference time interval makes the evaluation of the activity more precautionary for the subsequent evaluation of hazard, since the behavior of each landslide is analyzed within a wider time frame with respect to the 12-month-based observation range proposed by the WP/WLI in 1993. However, changes of the deformation behavior recorded at the end of a time period and indicative of movement reactivation may be blurred by the long history of motion recorded in the PS time series and may not be clearly recognized by simply using PS yearly velocities. Future development of advanced tools to better analyze PS deformation series will most likely contribute to better characterization and early detection of landslide accelerations or reactivations recorded within the monitored intervals.

Overlapping of PSI data with referenced landslide information

When the interval spanned by the available PSI-derived data temporally overlap with the date of completion of the preexisting inventory (e.g., 2003–2010 PSI data for the updating of a 2007 inventory, as for landslide L18 in Verbicaro), the PSI velocities do not represent just the deformational scenario subsequent to the time reference of the inventory itself (i.e. 2008–2010, for the above-mentioned example); they rather include some contributions from the scenario antecedent to this reference (i.e., 2003–2007). Previous PSI-based landslide studies and the application on Verbicaro used simple interpretation of full PS time series of ground deformation, regardless of this overlapping. Alternatively, advanced postprocessing PSI products obtained through the temporal subsampling of PSI deformation histories—as those recently exploited by Cigna et al. (2011)—may be considered to solve this temporal inconsistency. In particular, subsampled yearly deformation velocities might be derived by analyzing long-term PS time series and recalculating average rates in the time period subsequent to the reference year of the available preexisting inventory, i.e., separating the deformation velocities pre- and postinventory (for the above-mentioned example, 2003–2007 and 2008–2010 data, respectively). In some cases, however, this approach is strongly influenced by some parameters employed during the PSI processing, such as the model chosen to unwrap phase variations through time (generally, linear); thus, the whole PS time series (both pre- and postinventory) may be already intrinsically influenced by the entire deformation history of the analyzed time span.

Choice of activity and intensity thresholds

The choice of activity and intensity thresholds is a key point for the PSI-based matrix analysis and needs to be performed taking into account the following facets:

– Typology of observed deformation processes (e.g., geometry and expected velocity);
– Technical characteristics of available PSI data (e.g., LOS orientation);
– Postprocessing steps carried out during the evaluation of landslide representative velocities (e.g., reprojection or not of LOS estimates to most probable directions of movement; V_{ACT} and V_{INT} will be lower for LOS values than for reprojected data, as shown for the Verbicaro case study).

Usually, V_{INT} is precautionarily assumed lower than the official velocity threshold discriminating extremely from very slow landslides (i.e., 16 mm/year; Cruden and Varnes 1996). This choice is mainly driven by the frequent assumption of average velocities as the representative rates of movement for the analyzed phenomena; maximum deformation rates (peak velocities; Cruden and Varnes 1996) may significantly exceed the averaged patterns of the whole landslide, since displacement rates usually differ (spatially) within the same landslide area. Moreover, the temporal variations of ground displacements should also be considered; PSI-derived data are evaluated as averages of observations over long time periods (several years) and they are, therefore, expected to be lower than peak velocities (as also recently observed by Cascini et al. 2010).

If neither a reprojection of LOS velocities along the slope direction nor the combination of ascending and descending estimates are applied, the use of lowered thresholds might affect the results of the implementation for those phenomena moving approximately close to the direction of the employed LOS (Bianchini et al. 2012). For these landslides, the exploitation of low thresholds results in an overestimation of the landslide velocities—and consequently, the respective intensity—, since these phenomena are classified as faster than they really are.

With regard to V_{ACT}, the choice of the minimum value exceeding the precision of the PSI technique, i.e., a few millimeter per year, is usually performed (e.g., Cascini et al. 2010; Meisina et al. 2006, 2008). The implementation of the methodology for Verbicaro showed also how this value may be converted to account for the projection of LOS velocity along the slope directions. Differently from other applications, this conversion entails the use of higher thresholds for discriminating states of activity and intensities in order to account for the lower underestimation of real velocities occurring with the use of SLOPE-projected values with respect to that attributed to LOS velocities.

Another approach to calibrate the activity threshold might use training data—for which ground truth or in situ data are available—and then apply the determined threshold to the entire zone of interest. To this aim, historical PSI data (e.g., ERS 1992–2001 data) and past field-based activity determinations (past landslide inventory; e.g., map referenced 2001) may also be used, respectively, as training inputs and outputs for the determination of the activity using the PSI data. Operatively, for some training areas, the updating of the landslide activity can be simulated, starting from the determination of landslide representative velocities by using PSI data and then testing different thresholds to determine the landslide states of activity. The appropriate activity threshold for the area can then be chosen as the value producing the highest number of correspondences between simulated activity determinations (based on PSI data) and field-based evaluations.

As pointed out by Bianchini et al. (2012), the use of significantly low activity thresholds (e.g., a few millimeter per year) reduces the probability of discarding movements potentially critical, guaranteeing that even the slower motions are detected and classified. However, it causes some gravitational movements, such erosion, seasonal, or continuous downhill creep, to be included in the updated inventory maps.

Need of field validation

The PSI-based matrix approach, as any landslide study supported by remote sensing data, should always be validated through field checks and surveys in order to confirm, or even improve, all the information and evaluations performed through satellite radar interpretation to verify damage on buildings and infrastructure and other geomorphologic indicators and features induced by ground instability (e.g., Meisina et al. 2008; Righini et al. 2011). The need of field checks is also induced by those ambiguous classifications of the states of activity included in the activity matrices (e.g., what happened for landslide L23 in Verbicaro), for which on-site inspections are required to confirm an actual lowering of the landslide activity. Anyhow, it is clear that PSI-based landslide studies facilitate the scanning of very large areas to identify hotspot zones on which on-site checks and surveys have to be prioritarily carried out, focusing field investigations on the areas of (potentially) higher risk and thus significantly reducing efforts, times, and costs of on site activities (Bianchini et al. 2012).

Conclusions

We presented the definition, procedures, discussion, and one example of application of the 'PSI-based matrix approach', a methodology employed for the assessment or updating of the state

of activity and intensity of extremely to very slow landslide processes. For the case study of Verbicaro, we exploited 1992–2011 PSI data, and the methodology allowed the assessment of the state of activity and the intensity for 13 of the 24 premapped phenomena and also for the two newly identified phenomena, L25 and L26, with the year 2011 or 2010 as temporal reference of these estimations. For the remaining 11 landslides, the activity recorded in 2007 in the IFFI inventory was confirmed, and no evaluation of the intensity was performed due to the absence or insufficiency of PS data within the boundaries of these phenomena. Considering both premapped and newly identified phenomena, four reactivated (*R*), 18 active (*A*), three dormant (*D*), and one dormant/stabilized (*D/S*) landslides were finally identified; as for intensity, the distribution showed 13 very slow (VS), one extremely slow (ES), one negligible (*N*), and 11 not classified (NC).

Both the application for the test area of Verbicaro and past landslide investigations brought to light the major influencing factors of the PSI-based matrix approach, such as the lack of PS data within the landslide boundaries, the temporal coverage of the available data, and the need of field checks and validation as well as the operative procedures to choose the activity and intensity thresholds. Further improvements of the methodology will surely follow in the upcoming years as a consequence of the use of high spatial and temporal resolution imagery acquired by new satellites as well as the development of advanced approaches for the postprocessing analysis of PS data and in-depth exploitation of the information stored within the PS time series.

References

Amodio Morelli L, Bonardi G, Colonna V, Dietrich D, Giunta G, Ippolito F, Liguori V, Lorenzoni S, Paglionico A, Perrone V, Piccarretta G, Russo M, Scandone P, Zanettin Lorenzoni E, Zuppetta A (1976) L'arco Calabro-Peloritano nell'orogene Appenninico-Maghrebide. Mem Soc Geol Ital 17:1–60

Antonello G, Casagli N, Farina P, Leva D, Nico G, Sieber AJ, Tarchi D (2004) Ground-based SAR interferometry for monitoring mass movements. Landslides 1(1):21–28

Bianchini S, Cigna F, Righini G, Proietti C, Casagli N (2012) Landslide hotspot mapping by means of persistent scatterer interferometry. Environ Earth Sci. doi:10.1007/s12665-012-1559-5

Bovenga F, Nutricato R, Refice A, Wasowski J (2006) Application of multi-temporal differential interferometry to slope instability detection in urban/peri-urban areas. Eng Geol 88:219–240

Canuti P, Focardi P (1986) Slope stability and landslides investigation in Tuscany. Mem Soc Geol Ital 31:307–315

Carrara A, Merenda L (1976) Landslide inventory in northern Calabria, southern Italy. Geol Soc Am Bull 87:1153–1162

Cascini L, Fornaro G, Peduto D (2010) Advanced low- and full-resolution DInSAR map generation for slow-moving landslide analysis at different scales. Eng Geol 112:29–42

Cigna F, Del Ventisette C, Liguori V, Casagli N (2011) Advanced radar-interpretation of InSAR time series for mapping and characterization of geological processes. Nat Hazards Earth Syst Sci 11(3):865–881

Colesanti C, Wasowski J (2006) Investigating landslides with space-borne synthetic aperture radar (SAR) interferometry. Eng Geol 88:173–199

Colombo A, Mallen L, Pispico R, Giannico C, Bianchi M, Savio G (2007) Mappatura regionale delle aree monitorabili mediante l'uso della tecnica PS. In: Proceedings of 10° National Conference ASITA, Bolzano, Italy, 14–17 November 2006

Costantini M, Iodice A, Magnapane L, Pietranera L (2000) Monitoring terrain movements by means of sparse SAR differential interferometric measurements. In: Proceedings of IGARSS 2000, 20th IEEE International Geoscience and Remote Sensing Symposium, Honolulu, Hawaii, USA, 24–28 July 2000, pp 3225–3227

Crosetto M, Monserrat O, Iglesias R, Crippa B (2010) Persistent scatterer interferometry: potential, limits and initial C- and X-band comparison. Photogramm Eng Remote Sens 76(9):1061–1069

Cruden DM, Varnes DJ (1996) Landslide types and processes. In: Turner AK, Schuster RL (eds) Landslides: investigation and mitigation, Sp. Rep. 247, Transportation Research Board, National Research Council. National Academy, Washington DC, pp 36–75

Cucci L, Cinti FR (1998) Regional uplift and local tectonic deformation recorded by the Quaternary marine terraces on the Ionian coast of the northern Calabria (southern Italy). Tectonophys 292:67–83

Farina P, Colombo D, Fumagalli A, Marks F, Moretti S (2006) Permanent scatterers for landslide investigations: outcomes from the ESA-SLAM project. Eng Geol 88:200–217

Fell R, Corominas J, Bonnard C, Cascini L, Leroi E, Savage WZ (2008) Guidelines for landslide susceptibility, hazard and risk zoning for land use planning. Eng Geol 102:85–98

Ferranti L, Santoro E, Mazzella ME, Monaco C, Morelli D (2009) Active transpression in the northern Calabria Apennines, southern Italy. Tectonophys 476:226–251

Ferretti A, Prati C, Rocca F (2001) Permanent scatterers in SAR interferometry. IEEE Trans Geosci Remote Sens 39(1):8–20

Gonzalez-Diez A, Remondo J, Diaz de Teràn R, Cendrero A (1999) A methodological approach for the analysis of the temporal occurrence and triggering factors of landslides. Geomorphol 30:95–113

Greif V, VIcko J (2011) Monitoring of post-failure landslide deformation by the PS-InSAR technique at Lubietova in Central Slovakia. Environ Earth Sci. doi:10.1007/s12665-011-0951-x

Guzzetti F, Carrara A, Cardinali M, Reichenbach P (1999) Landslide hazard evaluation: a review of current techniques and their application in a multi-scale study, Central Italy. Geomorphol 31:181–216

Hanssen RF (2005) Satellite radar interferometry for deformation monitoring: a priori assessment of feasibility and accuracy. Int J Appl Earth Obs 6:253–260

Herrera G, Notti D, García-Davalillo JC, Mora O, Cooksley G, Sánchez M, Arnaud A, Crosetto M (2010) Landslides analysis with C- and X-band satellite SAR data: the Portalet landslide area. Landslides 7:1–12

Hilley GE, Bürgmann R, Ferretti A, Novali F, Rocca F (2004) Dynamics of slow-moving landslides from permanent scatterer analysis. Science 304(5679):1952–1955

Hungr O (1997) Some methods of landslide intensity mapping. In: Cruden D, Fell R (eds) Landslide risk assessment, Proceedings of the International Workshop on Landslide Risk Assessment, Honolulu, USA, February 19–21, 1997. Balkema, Rotterdam, pp 215–226

Iannace A, Bonardi G, D'Errico M, Mazzoli S, Perrone V, Vitale S (2005) Structural setting and tectonic evolution of the Apennine Units of northern Calabria. C R Geoscience 337:1541–1550

Lateltin O, Haemmig C, Raetzo H, Bonnard C (2005) Landslide risk management in Switzerland. Landslides 2(4):313–320

Meisina C, Zucca F, Fossati D, Ceriani M, Allievi J (2006) Ground deformation monitoring by using the permanent scatterers technique: the example of the Oltrepo Pavese (Lombardia, Italy). Eng Geol 88:240–259

Meisina C, Zucca F, Notti D, Colombo A, Cucchi A, Savio G, Giannico C, Bianchi M (2008) Geological interpretation of PSInSAR data at regional scale. Sensors 8(11):7469–7492

Notti D, Davalillo JC, Herrera G, Mora O (2010) Assessment of the performance of X-band satellite radar data for landslide mapping and monitoring: Upper Tena Valley case study. Nat Hazards Earth Syst Sci 10:1865–1875

Parise M, Wasowski J (1999) Landslide activity maps for landslide hazard evaluation: three case studies from Southern Italy. Nat Hazards 20(2):159–183

Righini G, Pancioli V, Casagli N (2011) Updating landslide inventory maps using persistent scatterer interferometry (PSI). Int J Remote Sens. doi:10.1080/01431161.2011.605087

Savio G, Ferretti A, Novali F, Musazzi S, Prati C, Rocca F (2005) PSInSAR™ validation by means of a blind experiment using dihedral reflectors. In: Proceedings of FRINGE 2005, Frascati, Italy, 28 November–2 December 2005, pp 1–6

Uzielli M, Nadim F, Lacasse S, Kaynia AM (2008) A conceptual framework for quantitative estimation of physical vulnerability to landslides. Eng Geol 102:251–256

Van Dijk JP, Bello M, Brancaleoni GP, Cantarella G, Costa V, Frixa A, Golfetto F, Merlini S, Riva M, Torricelli S, Toscano C, Zerilli A (2000) A regional structural model for the northern sector of the Calabrian Arc (Southern Italy). Tectonophys 324:267–320

Werner C, Wegmuller U, Strozzi T, Wiesmann A (2003) Interferometric point target analysis for deformation mapping. In: Proceedings of IGARSS 2003, 23rd IEEE International Geoscience and Remote Sensing Symposium, Toulouse, France, 21–25 July 2003, pp 4362–4364

Wieczorek GF (1984) Preparing a detailed landslide-inventory map for hazard evaluation and reduction. IAEG Bull 21(3):337–342

WP/WLI—Working Party on World Landslide Inventory (1993) Multilingual glossary for landslides. The Canadian Geotechnical Society, BiTech, Richmond BC

F. Cigna · S. Bianchini · N. Casagli
Department of Earth Sciences,
University of Firenze,
Via La Pira 4, 50121 Firenze, Italy

Present Address:
F. Cigna (✉)
British Geological Survey,
Nicker Hill, Keyworth, NG12 5GG Nottingham, United Kingdom
e-mail: fcigna@bgs.ac.uk
e-mail: francesca.cigna@gmail.com